Available online at www.sciencedirect.com
ScienceDirect
Carbohydrate Research 342 (2007) 1333–1342
Carbohydrate RESEARCH

Impact of the extrusion process on xanthan gum behaviour

Nuno M. Sereno,* Sandra E. Hill and John R. Mitchell

Division of Food Sciences, School of Biosciences, University of Nottingham, Sutton Bonington Campus, Loughborough LE12 5RD, UK

Received 26 January 2007; received in revised form 12 March 2007; accepted 22 March 2007
Available online 28 March 2007

Abstract—Processing xanthan gum by extrusion and subsequent drying produces a biopolymer showing particulate, rather than molecular behaviour in aqueous solution. This form of xanthan disperses very readily to give a viscosity that is strongly dependent on salt concentration. On heating above the temperature of the order–disorder transition as determined by calorimetry, there is a viscosity transition that is indicative of the irreversible loss of the particulate structure. It is suggested that the extrusion process melts and aligns xanthan macromolecules. On cooling reordering will occur but in the highly concentrated environment in the extruder (≈45% water w/w), inter-molecular association between neighbouring macromolecules cannot proceed to completion due to kinetic trapping. As a consequence a network structure is created maintained by associations involving ordered regions. A xanthan solution can be prepared from this particulate material by dispersing and subsequent heating far more readily than can be achieved with non-processed xanthan.

Keywords: Xanthan gum; Extrusion; Rheology; Viscosity; Hydration; Xanthan gum particles

1. Introduction

Xanthan gum is produced by aerobic fermentation of a pure culture of the bacterium *Xanthomonas campestris*.[1] The structure of the polysaccharide is composed of a cellulose backbone, with trisaccharide side chains having the structure β-D-Manp-(1→4)-β-D-GlcAp-(1→2)-α-D-Manp-(1→ linked at C-3 on alternating anhydroglucose units.[2] Some of the terminal Man units have pyruvic acid attached as a 4,6-linked ketal and the inner Man is partially acetylated at C-6.[3,4] Molecular weights of xanthan gum have been reported to be in the order of 10^6 g/mol.[5–8]

At low temperatures xanthan gum exists in solution as an ordered helical structure stabilised by non-covalent bonds. For many years there has been some controversy as to whether this network assembly consists of side by side single helices[9] or coaxial double helices.[10] With the rise in temperature to a defined temperature (T_m), this ordered structure breaks down and there is a conformation transition to a more flexible molecular coil. The onset of the melting transition, as well as its temperature range, is mainly dependent on: the concentration of the polymer,[11,12] the ratio of acetyl and pyruvate groups[13,14] and the ionic strength of the system.[15–18] Even with its helical structure lost, the xanthan gum molecules still remain highly extended, possibly because of intra-molecular steric or electrostatic interactions[16] thus conserving some of the initial solution viscosity.

It is too simplistic to consider most solutions of commercial xanthan gum as molecularly dispersed helical dimers or disordered coils. It is now recognised that xanthan gum solutions frequently contain 'microgels'. These are small swollen aggregates of molecules, which can be observed using atomic force microscopy.[19,20] It has been suggested that these structures make an important contribution to the solution rheology and for most xanthan gum industrial applications their presence is acceptable. It has been suggested that the microgels are a consequence of several molecules being linked together with regions of helical dimers forming the junction zones.[20] The extent that such will happen will

* Corresponding author. Tel.: +44 (0)115 951 6198; fax: +44 (0)115 951 6142; e-mail: nuno.sereno@nottingham.ac.uk

0008-6215/$ - see front matter © 2007 Elsevier Ltd. All rights reserved.
doi:10.1016/j.carres.2007.03.023

depend on the recovery conditions from the fermentation broth.

A major issue in using xanthan gum for industrial applications is the difficulty in producing a homogenous dispersion. This is a concern with many hydrocolloids and is the result of entanglements between partly hydrated macromolecules, resulting in a gel like layer at the surface preventing separation of powder particles and hence ingress of water. As a consequence, high shear mixers are required and viscosity growth is seen over a long time period after initial mixing, due to the slow dissolution. There is substantial information, particularly in the patent literature, on methods of improving xanthan gum dispersibility. These include production of agglomerate structures, addition of surfactants and crosslinking with glyoxal.[21–26]

We have previously reported that by processing xanthan by twin-screw extrusion cooking under mild conditions, it is possible to produce a material, which disperses far more readily than other non-chemically modified xanthans.[27] The objective of the work described in this paper was to understand the structural origin of this improved dispersibility.

2. Results and discussion

2.1. Effect of processing on xanthan gum water dispersibility and viscosity

The improvement in the dispersibility of xanthan gum following extrusion processing was substantial as can be seen in Figure 1, which displays the appearance of processed and non-processed xanthan prepared to give a concentration of 0.75% in distilled water after 10 s of gentle hand mixing. The processed xanthan gum swells,

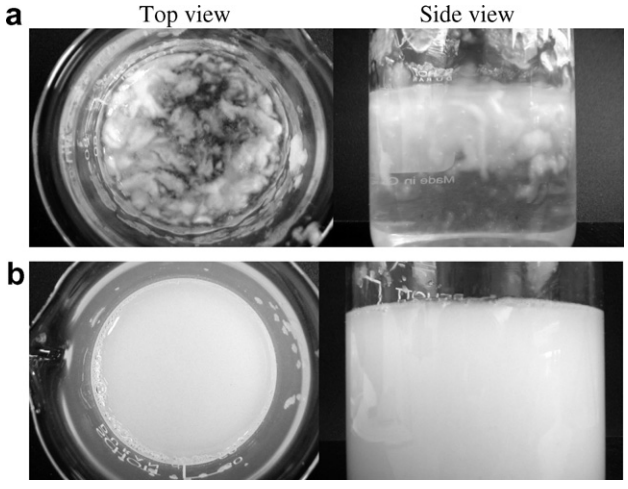

Figure 1. Xanthan gum dispersion in distilled water (0.75% wet weight basis): (a) non-processed xanthan gum and (b) extruded xanthan gum (dispersions prepared by mixing with a spoon for 10 s).

Table 1. Brookfield viscosity (Pa s) measurements of xanthan gum dispersions (0.75%, wet weight basis), which were mixed for 1 and 20 min at 300 rpm

Material	Mixing time (min)	
	1	20
Non-processed xanthan	0.103	1.16
Extruded xanthan	7.83	7.77

allowing an apparently homogeneous dispersion to be achieved even with minimal shear, in sharp contrast to the controlled material. Table 1 shows that the viscosity of the processed material is much higher than that of non-processed xanthan after one minute of mechanical mixing, and unlike the latter its viscosity remains stable over the 20 min mixing period.

Figure 2 displays the flow curves determined in distilled water, as a function of concentration and shear rate. The extruded material showed a much higher concentration dependence at higher concentrations than the non-processed xanthan gum. Also whereas a Newtonian plateau at low shear rates is apparent for the fully hydrated control material, this is not apparent for the extruded material. The lack of a low shear Newtonian plateau seems to suggest that the extruded system consists of a suspension of swollen particles rather than a polymer solution.

To support this hypothesis, the hydration of particles of processed and control xanthan gum was visualised under the optical microscope. The non-processed xanthan gum particle when in contact with excess water presented a very quick initial wetting (first 30 s), followed by a more gentle hydration during the next minute and a half and an eventual dissolution (Fig. 3a). A similar behaviour has also been observed by Clark.[28] Figure 3b shows a very different behaviour for the extruded xanthan gum particle. Again, as observed for non-processed xanthan gum, an almost immediate water penetration into the dry particle occurred and caused a rapid increase in volume (first 30 s), but now the swollen particle remained stable without a change in size over the period of observation.

2.2. Effect of salt on viscosity dispersion behaviour

Some further insight into the origin of this behaviour can be obtained from determining the effects of salt concentration on viscosity. As can be observed in Figure 4 both forms of xanthan gum, although displaying a clear shear-thinning behaviour, show a very different response to NaCl concentration. The non-processed xanthan gum dispersions showed a small increase in viscosity with the addition of NaCl. This rheological response was expected for the non-processed xanthan gum system when in the semi-dilute regime. The addition of salt is responsible for shielding the ionic groups on the xan-

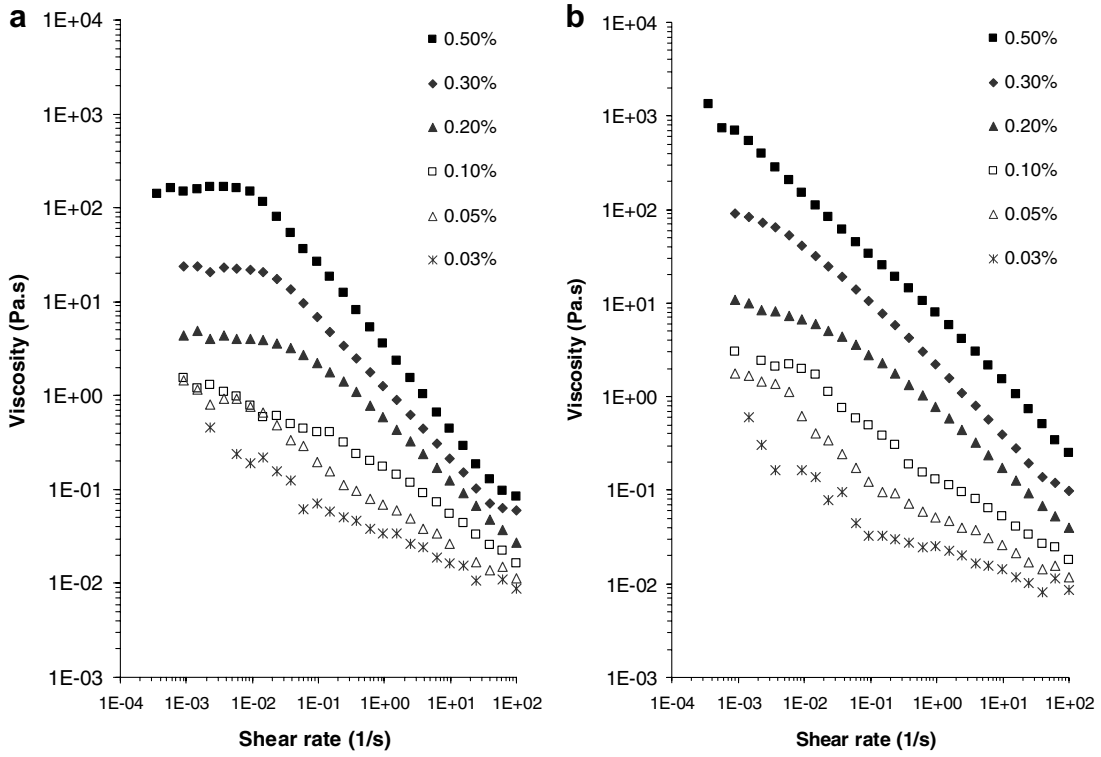

Figure 2. Viscosity of distilled water dispersions containing xanthan gum at different concentrations (%, wet weight basis): (a) non-processed xanthan gum and (b) extruded xanthan gum. Measurements were performed in the Bohlin CVO-R.

than side chains. This causes a reduction of individual molecular volume occupancy, but also promotes an increase in molecular entanglements in the dispersion, leading to an increase in viscosity.[29] In the semi-dilute system this latter situation will be more significant,[15] and the system viscosity will increase with increasing NaCl concentration. Above 0.1%, further addition of NaCl had little effect on dispersion viscosity (Fig. 4a). This salt dependence followed a very different pattern for the extruded material, which showed a substantial viscosity decrease with increasing NaCl levels (Fig. 4b). Moreover, only at low salt levels and moderate to high shear forces, conditions close to those of the Brookfield tests presented in Table 1, the extruded xanthan gum systems gave substantially higher viscosities than the non-processed xanthan gum dispersions.

The strong ionic strength dependence on viscosity is a consequence of the reduction in the degree of swelling of the particles with salt concentration. This can be clearly observed under the microscope (data not shown), and can be quantified by measuring the volume of the particulate phase following separation by centrifugation as a function of salt concentration. The swelling mass ratio (Q), for a dispersion of 0.75% (wet weight basis) extruded xanthan gum in distilled water was 1110 ($g_{swelling}/g_{dry\ xanthan}$), which decreased by about 40 times when determined in the presence of a 1.0% NaCl solution (Fig. 5).

The strong salt dependence on the particle volume explains the viscosity dependence on salt concentration shown in Figure 4b. The individual particles behave as polyelectrolyte gels. It is recognised that swelling of these gels will be determined primarily by a balance between osmotic pressure of the free ions, which can be understood in terms of Donnan equilibrium, and an elastic retractive force.[30] The strong salt dependence of the Donnan term is responsible for the observed swelling behaviour. A more precise theoretical understanding in this case is complicated by the non-Gaussian nature of the xanthan gum chains, which in the ordered form have persistence length ≈100 nm.[8]

Although a restriction in swelling was observed in the presence of salt, it was not clear at this point if the particle integrity would be kept when NaCl was added to an already fully swollen particle. Figure 6 clearly depicts that on addition of a NaCl solution to give a final NaCl concentration of 1% to a particle first swollen in distilled water, the particle shrinks and maintains its cohesion. The darker regions created at the end of the test indicated an increase in density, which suggests that the polymer remained inside the xanthan swollen particle and was not substantially released into the aqueous solution. To confirm this, measurements were made of the xanthan concentration in the supernatant following centrifugation both by polyelectrolyte titration and the more conventional phenol sulfuric acid method.[31]

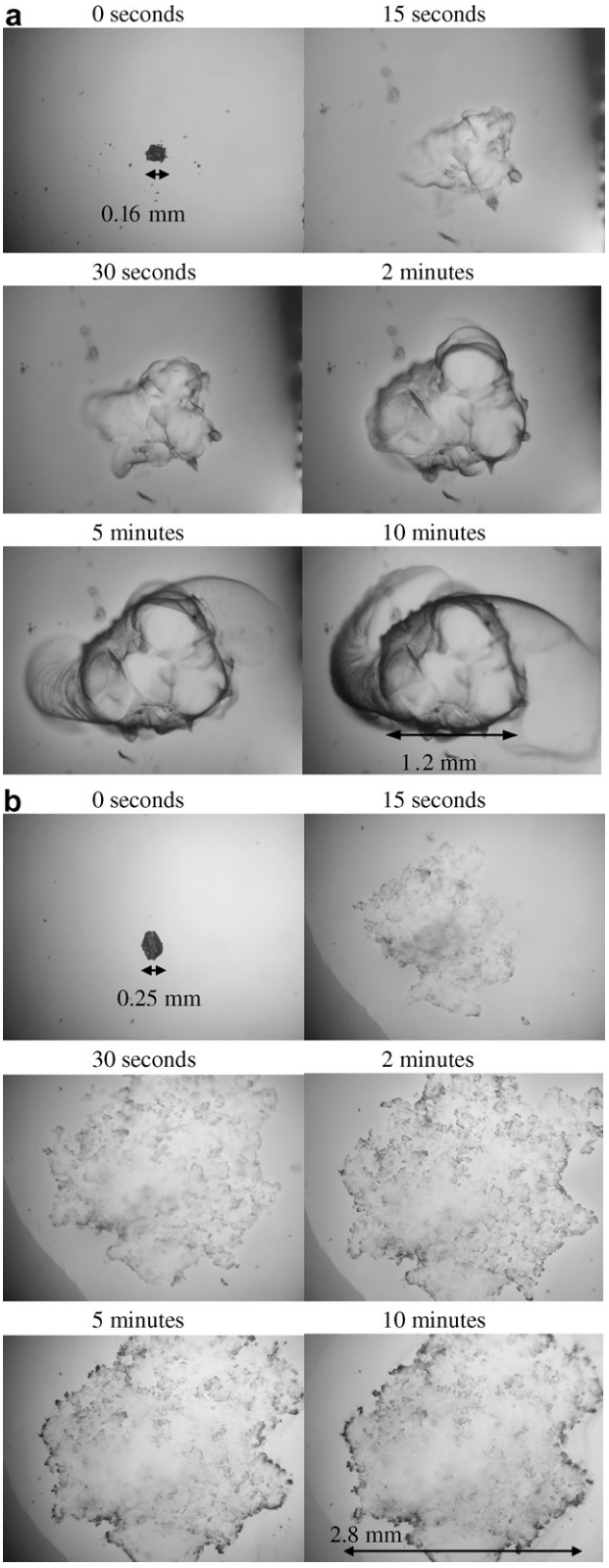

Figure 3. Hydration in distilled water of (a) non-processed xanthan gum and (b) extruded xanthan gum.

Quantitative information on xanthan gum partition between the particulate phase and the solvent was obtained.

These results presented in Table 2 show good agreement between the two methods and confirm that at least 75% of the extruded material remains in the particulate form, even when submitted to paddle shears forces of ≈750 rpm for 30 min with subsequent centrifugation at 4000 rpm for ≈2 h. It also appeared that the increased ionic strength had the ability to decrease xanthan molecular leakage from the granule to the solution. This reinforces the view that increasing ionic strength promotes higher levels of molecular interactions, which therefore allowed for less leakage from the particles. It is also possible that the larger swollen particles at lower salt levels were more susceptible to disruption on centrifugation. The maintenance of the majority of the processed xanthan gum in the particulate form explains its good dispersibility, since entanglements between molecules partly released from powder particles is reduced when compared with non-processed xanthan.

2.3. Temperature induced transition

To determine the role of ordered structure in maintaining the integrity of the xanthan particles the temperature and enthalpy of melting and reforming of the ordered structure were compared for the two xanthan systems. Figure 7 displays the effect of salt and temperature on the viscosity of extruded xanthan gum measured with the rapid viscosity analyser (RVA). Firstly, it can be seen that the substantial difference in low temperature viscosity and rheological behaviour between the two xanthan gum systems without salt is confirmed. Secondly for the lower temperatures the strong salt dependence of the extruded xanthan reported in Figure 4 is again seen. With the addition of small amounts of salt ($\leqslant$0.01%) an increase in low temperature viscosity was observed. It appears that the low salt levels do not affect particle swelling, but enhance particle rigidity by enhancing molecular interactions due to shielding of electrostatic repulsions (as shown by polyelectrolyte titration). With the rise in temperature there was a transition, which was characterised by a viscosity decrease at low NaCl concentrations or as a viscosity peak at higher NaCl concentrations. The transition shifted to higher temperatures as NaCl concentration in the system increased.

It is tempting to associate the viscosity transitions observed with the well known salt dependent xanthan gum order–disordered transition. In order to obtain evidence to support this hypothesis this transition was followed by microcalorimetry. Figure 8 shows that NaCl up to concentrations of 0.7% altered the transition temperature of both non-processed and extruded xanthan gum dispersions to a similar extent. On cooling from above the melting temperature (T_m), an exothermic transition was observed suggesting the reforming of the xanthan gum structure. The cooling enthalpies also demon-

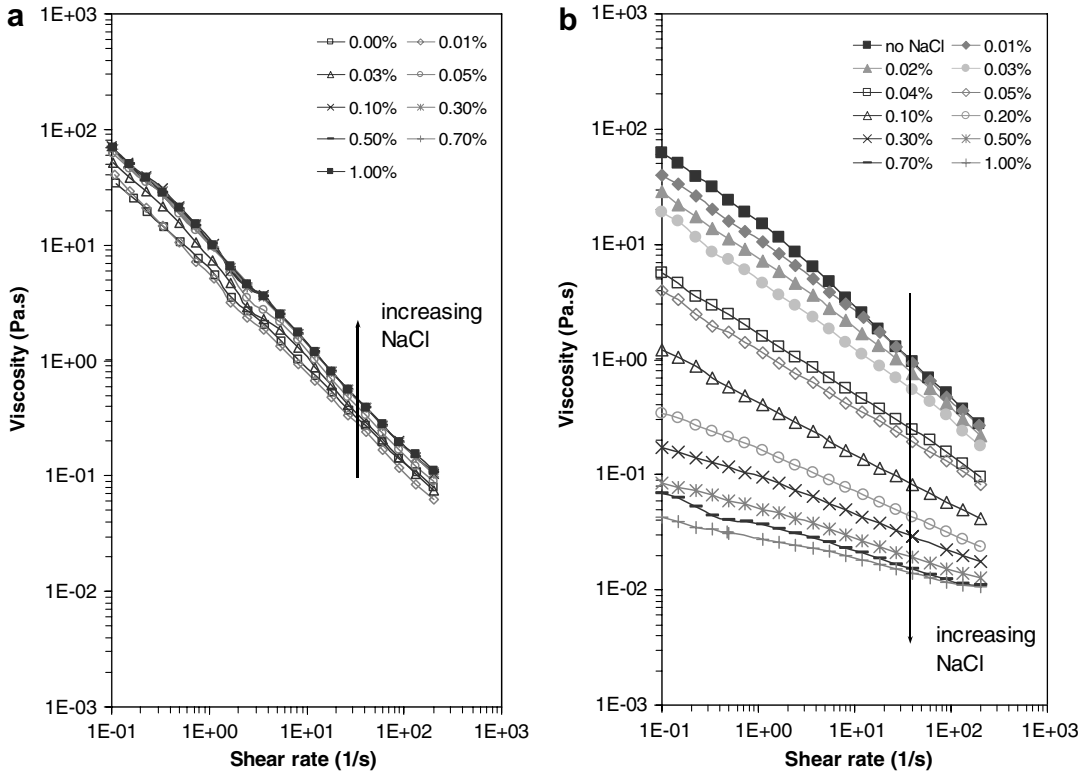

Figure 4. Viscosity of 0.75% (wet weight basis) xanthan gum dispersions at different NaCl concentrations: (a) non-processed xanthan gum and (b) extruded xanthan gum. Measurements were performed in the Bohlin CVO.

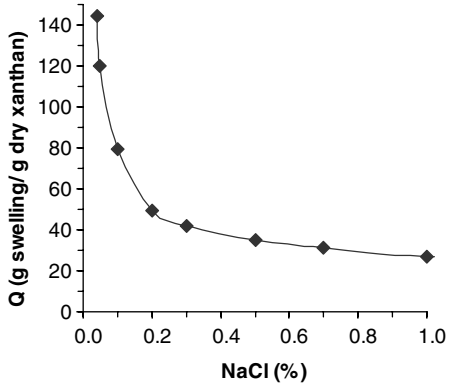

Figure 5. Swelling mass ratio of extruded xanthan gum dispersions (0.75%, wet weight basis) prepared at different NaCl concentrations.

strated the reversible nature of the extruded gum. At higher salt concentrations it is possible to compare the temperature for maximum viscosity, with the peak temperature from the heating endotherms of processed xanthan (Fig. 9). The similarity between the two temperatures supports the hypothesis that the particulate nature of xanthan gum is maintained by the junction zones of the type existing in the ordered form of 'molecular' xanthan. The lower peak viscosity temperature compared with the calorimetry temperature, at the lower salt concentrations, probably reflects the disruption/dissolution of some swollen particles at temperatures below the disruption of the majority of the ordered regions.

Even though the onset and extent of the thermal transition of the two systems was similar, the energies involved in the initial endothermic melting were much lower for the extruded xanthan gum system compared with the non-processed material (Fig. 8). Such differences were seen over the whole salt range, but were more pronounced at low salt levels. The enthalpy value for the extruded xanthan gum systems was $\approx$5.7 J/$g_{xanthan}$ compared with 9.9 J/$g_{xanthan}$ for the non-processed material. On cooling the differences in enthalpy between both xanthan systems were smaller (Fig. 8). On subsequent re-heating in distilled water no substantial differences were observed between the two systems (Table 3).

The strong salt dependence for the melting enthalpy of the processed system could reflect some disruption of weak associates as a consequence of swelling in the lower salt environments. This is likely to be a consequence of both the lower stability of the ordered form and greater Donnan swelling at low salt concentrations. Disruption of some of these regions would explain the solubilisation of more of the polysaccharide from the particle with decreasing salt levels, as shown in Table 2. The presence of NaCl also affected the re-organisation of the xanthan gum structure on cooling from above T_m,

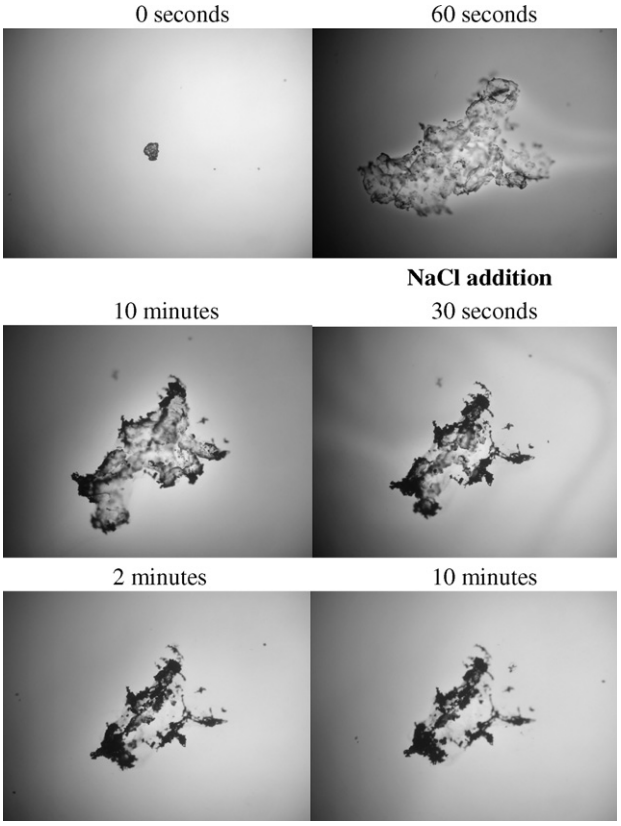

Figure 6. Hydration of extruded xanthan gum in distilled water, with subsequent addition of 1% NaCl after 10 min of hydration.

Table 2. Concentration of xanthan retained in particulate form of extruded xanthan gum dispersions (0.75%, wet weight basis) following centrifugation

NaCl (%)	Xanthan in particulate form (%)	
	(a)	(b)
0.00	76.4	—
0.10	88.4	88.9
0.50	93.3	93.4

Xanthan gum dispersions were prepared at different NaCl levels. Two methods were used: (a) polyelectrolyte titration method, (b) total sugar content method.[31]

resulting in a decrease in energy release as NaCl levels decreased. The reason for this behaviour can be explained through the NaCl ability to shield the electrostatic repulsion forces present on the xanthan gum side chains. This electrostatic repulsion is responsible for keeping the xanthan molecules separated and challenging the re-association, so its neutralisation means an easier re-association with greater energy release.

The small differences shown in Table 3 in the energy requirements for the melting endotherm and reordering exotherm for non-processed xanthan gum, have also been reported by Capron et al.[32] and Rochefort and Middleman.[17] These researchers suggested that when cooling from above T_m, differences in structural aggregation were observed resulting in assemblies, which differ from the original. It is then fair to believe that this anomaly is due to the rate of cooling from above the melting temperature (T_m), which has an influence on the conformation reordering of the xanthan helixes into single or double helical structures.[33]

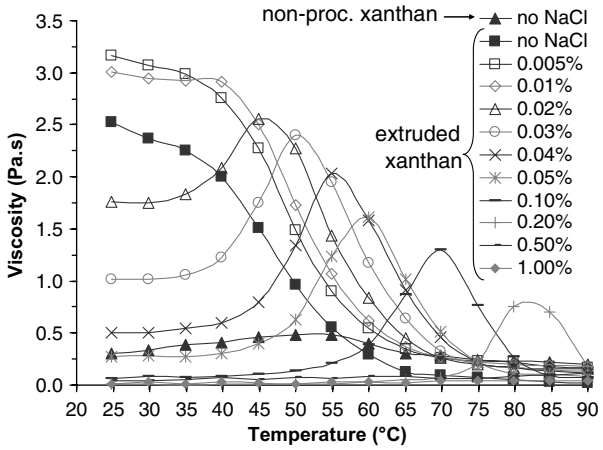

Figure 7. Viscosity measurement of non-processed xanthan gum (0.75%, wet weight basis) in distilled water and extruded xanthan gum (0.75%, wet weight basis) in NaCl solutions of increasing concentration. Measurements were performed in the Rapid Visco Analyser.

2.4. Model for the extruded xanthan gum molecular organisation

The combination of the hydration, viscosity and calorimetric measurements resulted in a possible hypothesis as to the structure of the extruded xanthan gum. As previously mentioned, the ordered conformation of xanthan gum is believed to be a helical structure. It is proposed that this original helical structure is lost inside the extruder, due to the high pressures and mechanical stress generated by the flowing of this highly viscous melt through the extruder barrel. On cooling due to the emergence from the extruder die a continuous network is formed, which is maintained by helical junction regions involving segments of different lengths. On subsequent drying and milling particles of crosslinked material are created. Once hydrated in cold water extruded xanthan gum instead of forming a molecular solution, forms particles, which behave as super-swelling polyelectrolyte gels.

The lower enthalpy of melting on heating suggest that the extruded xanthan gum particles possess a greater proportion of non-helical amorphous regions than the non-processed material. The suggested extruded xanthan gum structure is illustrated schematically in Figure 10.

At a certain temperature junction zones within the processed xanthan gum will melt causing the disruption of the particles. Therefore, once in this disordered state,

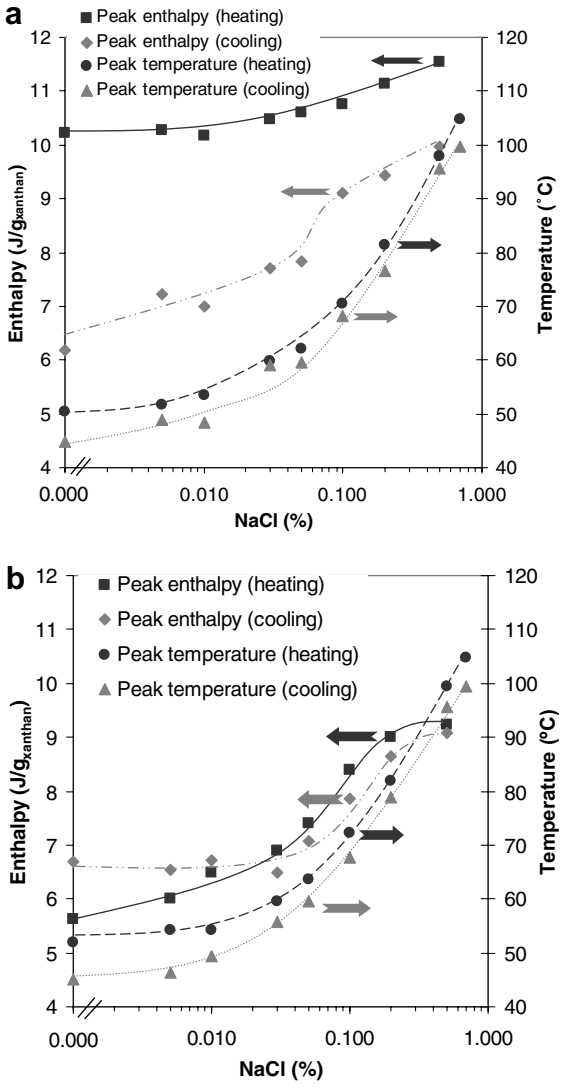

Figure 8. Enthalpy and temperature of the thermal transition observed on heating and cooling of a 0.75% (wet weight basis) dispersion of (a) non-processed xanthan gum and (b) extruded xanthan gum; in NaCl solutions of increasing concentration.

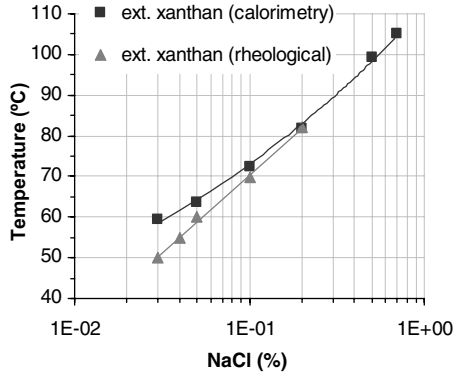

Figure 9. Mid-point of the thermal transition of extruded xanthan gum dispersions (0.75%, wet weight basis) in NaCl solutions, as observed by rheological and calorimetric methods.

Table 3. Xanthan gum's enthalpy of thermal transition in distilled water

Sample	Endothermic enthalpy ($J/g_{xanthan}$)	
	Heating	Re-heating
Non-processed xanthan gum dispersion		
1	9.6	8.1
2	10.2	7.7
Extruded xanthan gum dispersion		
1	5.7	7.9
2	5.7	8.6

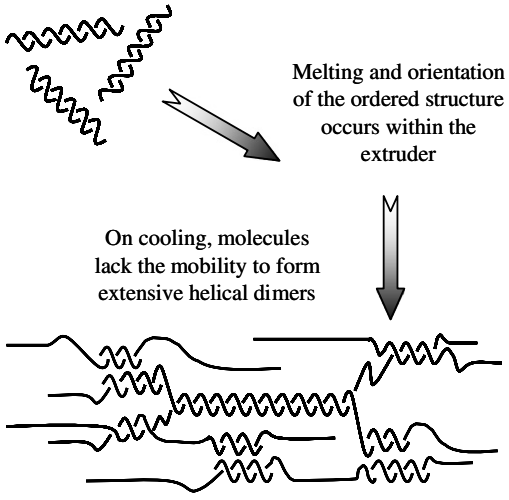

Figure 10. Model of xanthan gum molecular organisation resulting from extrusion and subsequent drying.

the extruded xanthan gum would show a similar molecular dispersion to the disordered non-processed material. On subsequent cooling below the melting temperature (T_m), both systems would go through a similar process of coil-helix re-association, which consists of the reassembly of the side chains to the backbone and reforming of a helical structure. This can be seen by the similarities in energy release on cooling shown by both systems (Fig. 8).

In has been suggested that precipitation and drying xanthan gum from fermentation broths at low salt levels, where the xanthan double helix is partly destabilised, leads to inter-molecular rather than intra-molecular helix formation, reduction in product solubility and an increase in microgel formation.[20] In the process described in this paper, network formation appears to be extensive and involving the majority of the material. The factors that we consider govern the degree of network formation are:

The melting temperature (T_m). This will depend not only on salt content, but also by analogy with the melting of other biopolymer systems, such as starch [34,35] and globular proteins denaturation,[36] on water content. At low

water contents, relevant to the extrusion and drying stages, the water content dependence will be expected to be severe.

Mobility. This will depend on the proximity of the non-ordered amorphous component to its glass transition temperature (T_g). A rapid approach to the glass transition temperature (T_g) with a subsequent reduction in mobility will result in: a reduction of the growth rate of double helical regions with respect to single helices, and also in kinetically trapped amorphous regions.

Orientation. The alignment of macromolecules in the extruder die could contribute to the disruption of order on heating and will influence the structure of the final partially reordered product.

In conclusion, our results show that a new type of xanthan gum with excellent dispersibility and unusual rheological behaviour can be prepared by twin-screw extrusion. The material behaves like particles of a cross-linked polyelectrolyte gel, with a very strong salt dependence on swelling and on dispersion viscosity. Particle integrity is the result of a network, maintained by helical junction zones. This different molecular assembly generated through extrusion, is dissipated on heating reverting to a disordered coil structure similar to a non-extruded xanthan gum solution above its conformation transition temperature.

3. Experimental

3.1. Extrusion

Xanthan gum (Satiaxane CX 910, Degusa Texturant Systems, France) was extruded with a Twin Screw Clextral BC12 Extruder (Clextral, Firmeny-Cedex, France), with co-rotating screws. A slit die of 1 mm × 30 mm was fitted to the barrel's exit. The extrusion conditions are presented in Table 4.

3.2. Post-extrusion treatment

The extruded xanthan gum was dried in a vacuum oven (Sanyo Gallenkamp PLC) at 65 °C for ≈72 h under a pressure of 100 Pa (final water content <8%). After drying the material was ground at room temperature using a Cyclotec mill fitted with a 250 μm sieve. The resulting material was then sieved (AS200 analytical sieve shaker, Retsh Gmbh & Co) to a particle size between 125 and 250 μm, and stored in closed jars. The final water content of the samples was lower than 8% wet weight basis.

Table 4. Extrusion conditions

Screw diameter	24 mm
Screw length	400 mm
Screw speed	100 rpm
Residential time inside the extruder barrel	40 s
Solid feed rate	3.50 kg/h
Solid water content (wet weight basis)	12.3%
Water flow rate	2.14 L/h
Total amount of water inside the barrel	2.57 kg/h
Temperature of the barrel heating zones from the feed end	85, 85, 70 °C

3.3. Viscosity

Viscosity of xanthan gum solutions was measured both by semi-empirical and fundamental methods. A comparison of viscosity at constant temperature (25 ± 1 °C) was performed using a Synchro-Lectric LVT Brookfield viscometer (Brookfield Engineering Laboratories Inc., Stoughton, MA, USA) with a rotational speed of 12 rpm. Due to the substantial differences in sample viscosity and instrument limitation a change in spindle was required between samples. A spindle no. 3 was used for extruded xanthan gum and a spindle no. 2 for the non-processed material. The hydration method comprised of introducing 500 mL of distilled water to a 1 L beaker, stirring with a four bladed impeller with a diameter of 5 cm, operating at a fixed rate of 300 rpm and adding the xanthan gum to give a concentration of 0.7% based on the dry weight. Viscosities were measured immediately after mixing had proceeded for 1 min and for 20 min.

Xanthan gum viscosity, as a function of temperature, was measured using a Rapid Visco Analyser (RVA) (Newport Scientific, Calibre Control International, Warrington, UK). This instrument is well suited for following temperature dependence of viscosity without the complications of water loss, since it was originally designed to follow starch gelatinisation. A 0.75% xanthan gum dispersion (wet weight basis) was prepared by adding the solid powder to distilled water and stirring at 700 rpm for 20 min. The resulting suspension was allowed to settle for 2 h in order to fully hydrate the samples, before 25 g of the dispersion was transferred to the RVA canister and tested. The speed/temperature profile used and criteria to ascertain viscosity are described in Hill and Sereno.[37] Such a profile consists of periodically varying the stirring speed (between 960 rpm for 20 s and 60 rpm for 40 s) while heating the system from 20 to 90 °C over a period of 14 min at constant rate. Viscosity was recorded at the end of each 40 s low speed stirring period. The high stirring speed stage of the cycle prevents possible clumping and settlement of particles arising at lower shear speeds.

The flow properties of fully hydrated xanthan gum dispersions were characterised using both the Bohlin CVO and CVO-R rotational rheometers (Malvern Instruments Ltd, Worcestershire, UK). The rheometers operated at 25 ± 0.1 °C. Xanthan gum dispersions were prepared at a range of salt and xanthan gum concentra-

tions, by adding the solid powders to distilled water and stirring at 700 rpm for 20 min. The resulting suspension was kept for a period of 24 h at 4 °C. Subsequent equilibration to 25 °C preceded testing under steady shear conditions. Two measuring geometries were used: cone and plate and double gap.

3.4. Microcalorimetry

0.75% xanthan gum dispersions' thermal transition (%, wet weight basis) at different NaCl concentrations (Fisher Scientific, Loughborough, UK) was followed using a Micro DSC III (Setaram, France). This technique allowed for a precise monitoring of the thermal events observed during heating from 20 to 120 °C and cooling back to 20 °C. A re-heat and re-cooing of the sample, under the same conditions followed. The Micro DSC III was operated at a fix rate of 1 °C/min. Baseline determination was performed using empty stainless steal pans in both cells. For sample testing, the empty pan in the sample cell was replaced by a similar pan containing a xanthan gum dispersions prepared according to the protocol used in the RVA testing.

3.5. Optical microscopy

Dry xanthan gum particles (125–250 μm) were placed on a standard glass microscope slide, and a solution of toluidine blue (5 mg/kg water) was carefully added. The studies used an optical light microscope (Wild Leitz GmbH, Wetzlar, Germany). Depending on the required magnification a 4× or 10× objective with 1× eyepiece was used. The images were recorded with a Nikon Coolpix 990 digital camera.

3.6. Swelling mass ratio determination

The swelling mass ratio (Q, $g_{swollen\ extrudate}/g_{dry\ extrudate}$) of extruded xanthan gum dispersed in different NaCl concentrated solutions was determined following centrifugation. Centrifugation of xanthan gum dispersions was performed on a Multex centrifuge (Multex MSE P522A, Crawley, UK) with a radius to inner tip of 140 mm and operating at 4000 rpm for 2 h (2500g).

3.7. Polyelectrolyte titration

Polyelectrolyte titration against polydimethyl diallyl ammonium chloride (0.001 N), was used to assay xanthan gum in the supernatant following centrifugation. The end point was determined as zero streaming potential measured in a Mutek PCD 03 apparatus (Mutek, Germany). The concentrations were calculated from xanthan gum calibration curves obtained both in distilled water, and in 0.5% NaCl. To validate this approach the results were compared with the total sugar content of the supernatant extracted from a 0.75% extruded xanthan gum dispersion in 0.1% and 0.5% NaCl solutions (%, wet weight basis). These were measured using the colorimetric method described by Dubois et al.[31]

References

1. Pettitt, D. J. In *Polysaccharides in Food*; Blanshard, J. M. V., Mitchell, J. R., Eds.; Butterworth: London, Boston, 1979; pp 263–282.
2. Jansson, P.-e.; Kenne, L.; Lindberg, B. *Carbohydr. Res.* **1975**, *45*, 275–282.
3. Cottrell, I. W.; Kang, K. S.; Kovacs, P. In *Handbook of Water-Soluble Gums and Resins*; Davidson, R. L., Ed.; McGraw-Hill Book Company, 1980; pp 24.1–24.31.
4. Shatwell, K. P.; Sutherland, I. W.; Rossmurphy, S. B.; Dea, I. C. M. *Carbohydr. Polym.* **1990**, *14*, 29–51.
5. Milas, M.; Rinaudo, M. *Carbohydr. Res.* **1979**, *76*, 189–196.
6. Milas, M.; Viehweg, H.; Weiss, A. *Carbohydr. Polym.* **1990**, *13*, 119–131.
7. Dhami, R.; Harding, S. E.; Jones, T.; Hughes, T.; Mitchell, J. R.; To, K. M. *Carbohydr. Polym.* **1995**, *27*, 93–99.
8. Esquenet, C.; Buhler, E. *Macromolecules* **2002**, *35*, 3708–3716.
9. Norton, I. T.; Goodall, D. M.; Frangou, S. A.; Morris, E. R.; Rees, D. A. *J. Mol. Biol.* **1984**, *175*, 371–394.
10. Morris, V. J. In *Food Polysaccharides and Their Applications*; Stephen, A. M., Ed.; Marcel Dekker: New York, 1995; pp 341–376.
11. Challen, I. A. In *Food Hydrocolloids: Structure, Properties, and Functions*; Nishinari, K., Doi, E., Eds.; Plenum Press: New York and London, 1993; pp 135–140.
12. Milas, M.; Rinaudo, M.; Duplessix, R.; Borsali, R.; Lindner, P. *Macromolecules* **1995**, *28*, 3119–3124.
13. Callet, F.; Milas, M.; Rinaudo, M. *Int. J. Biol. Macromol.* **1987**, *9*, 291–293.
14. Shatwell, K. P.; Sutherland, I. W.; Dea, I. C. M.; Rossmurphy, S. B. *Carbohydr. Res.* **1990**, *206*, 87–103.
15. Symes, K. C. *Food Chem.* **1980**, *6*, 63–76.
16. Morris, V. J.; Franklin, D.; Ianson, K. *Carbohydr. Res.* **1983**, *121*, 13–30.
17. Rochefort, W. E.; Middleman, S. *J. Rheol.* **1987**, *31*, 337–369.
18. Marcotte, M.; Taherian, A. R.; Trigui, M.; Ramaswamy, H. S. *J. Food Eng.* **2001**, *48*, 157–167.
19. Gunning, A. P.; Kirby, A. R.; Morris, V. J. *Ultramicroscopy* **1996**, *63*, 1–3.
20. Morris, V. J.; Mackie, A. R.; Wilde, P. J.; Kirby, A. R.; Mills, E. C. N.; Gunning, A. P. *Lebensm. Wiss. Technol. Food Sci. Technol.* **2001**, *34*, 3–10.
21. Sandford, P. A.; Baird, J. K. U.S. Patent 4,357,260, 1982.
22. Cottrell, I. W.; Sandford, P. A.; Baird, J. K. U.S. Patent 4,363,669, 1982.
23. Baird, J. K.; Sandford, P. A. U.S. Patent 4,654,086, 1987.
24. Bernard, V. U.S. Patent 5,003,060, 1991.
25. Su, L.; Ji, W. K.; Lan, W. Z.; Dong, X. Q. *Carbohydr. Polym.* **2003**, *53*, 497–499.
26. Jampala, S. N.; Manolache, S.; Gunasekaran, S.; Denes, F. S. *J. Agric. Food Chem.* **2005**, *53*, 3618–3625.
27. Farhat, I. A.; Hill, S. E.; Mitchell, J. R.; Scharf, U.; Sereno, N. M.; Stolz, P. World Intellectual Property Organization WO/2006/065136A1, 2006.

28. Clark, R. In *Gums and Stabilisers for the Food Industry*; Williams, P. A., Phillips, G. O., Eds.; The Royal Society of Chemistry: Cambridge, UK, 2004; Vol. 12, pp 347–353.
29. Lee, H. C.; Brant, D. A. *Macromolecules* **2002**, *35*, 2223–2234.
30. Sasaki, S. *J. Chem. Phys.* **2006**, 124.
31. Dubois, M.; Gilles, K. A.; Hamilton, J. K.; Rebers, P. A.; Smith, F. *Anal. Chem.* **1956**, *28*, 350–356.
32. Capron, I.; Alexandre, S.; Muller, G. *Polymer* **1998**, *39*, 5725–5730.
33. Milas, M.; Rinaudo, M. *Carbohydr. Res.* **1986**, *158*, 191–204.
34. Biliaderis, C. G.; Maurice, T. J.; Vose, J. R. *J. Food Sci.* **1980**, *45*, 1669–1680.
35. Lund, D. B. In *Food Properties and Computer-Aided Engineering of Food Processing Systems*; Sing, R. P., Medina, A. G., Eds.; Kluwer Academic, 1989; pp 299–311.
36. Fujita, Y.; Noda, Y. *Bull. Chem. Soc. Jpn.* **1981**, *54*, 3233–3234.
37. Hill, S. E.; Sereno, N. *Newport Sci. World* **2005**, 1.